International Conference on Space Optics—ICSO 2022

Dubrovnik, Croatia

3–7 October 2022

Edited by Kyriaki Minoglou, Nikos Karafolas, and Bruno Cugny,

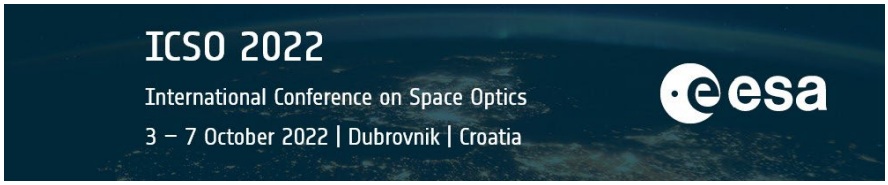

ESA Ground Infrastructure for the NASA/JPL PSYCHE Deep-Space Optical Communication Demonstration

International Conference on Space Optics — ICSO 2022, edited by Kyriaki Minoglou, Nikos Karafolas, Bruno Cugny, Proc. of SPIE Vol. 12777, 127770E · © 2023 ESA and CNES · 0277-786X · doi: 10.1117/12.2688805

ESA Ground Infrastructure for the NASA/JPL PSYCHE Deep-Space Optical Communication Demonstration

Daniel Rieländer[1], Andrea Di Mira[1], David Alaluf[2], Robert Daddato[1], Sinda Mejri[1], Jorge Piris[2], Jorge Alves[2], Dimitrios Antsos[3], Abhijit Biswas[3], Nikos Karafolas[2], Klaus-Jürgen Schulz[1] and Clemens Heese[1]
[1]ESA/ESOC, Robert-Bosch-Str. 5, 64295 Darmstadt.
[2]ESA/ESTEC, Keplerlaan 1, 2201 AZ Noordwijk, The Netherlands
[3]Jet Propulsion Laboratory, California Institute of Technology, 4800 Oak Grove Dr, Pasadena, CA 91109

ABSTRACT

The demonstration of interoperability of the deep-space optical ground demonstration infrastructures of the two space agencies, NASA and ESA, will reinforce optical communication for the use case of fast deep-space data return. The operational experience gained by this joint demonstration will enable future mission designers to efficiently trade the option of using optical communication as data-return vehicle for upcoming deep-space missions. ESA is investigating potential mission scenarios at Mars for which this technology demonstration and validation is considered essential.

In this paper ESA's ground demonstration infrastructure for optical data return from the Psyche mission is outlined. The deep-space mission to the asteroid Psyche will host a technology demonstration payload, the Deep Space Optical Communication (DSOC) system, developed by NASA. The mission's objective is to investigate the asteroid and its unique metallic surface. In addition to its primary objective, the mission will demonstrate an optical communication link between the spacecraft and earth with a separation of up to 2.5 AU. Here we provide link budget calculations for the data up- and the data downlink. Optical communication has the potential to deliver 10- to 100 times higher data rate compared to radio frequency, at lower size, weight and power consumption.

Keywords: Psyche, Optical Communication, Deep Space, Asteroid, DSOC Terminal, European, Ground Station, Demonstration, Single Photon Detection.

1. INTRODUCTION / DSOC TERMINAL

For this technology demonstration, ESA will develop an optical communication ground segment in Greece, which accompanies Nasa's ground segment in California. A ground laser transmitter and ground laser receiver will be deployed and used to transmit and receive data from the DSOC terminal on the Psyche spacecraft. The ground laser transmitter, described in section 2, provides modulation for data uplink on top of a beacon beam with up to 7 kW optical power at a wavelength of 1064 nm. It acts as an uplink channel with data rates in the kb/s range. The beacon mode ensures back-pointing of the spacecraft with arcsec-level precision. The ground laser receiver, described in section 3, will be based on the Aristarchos Telescope in Greece [1]. It will be equipped with a superconducting nanowire array optical detector. The high timing accuracy as well as the sensitivity of the detectors increase data rates and range. For the data transfer, the high-photon-efficiency, serially concatenated pulse position modulation (SC-PPM [2]) protocol will be employed. In this modulation scheme, the bits are encoded by the temporal 'position' of a pulse within a timeframe. The objective is to demonstrate inter-operability between Agency's ground demonstration infrastructures.

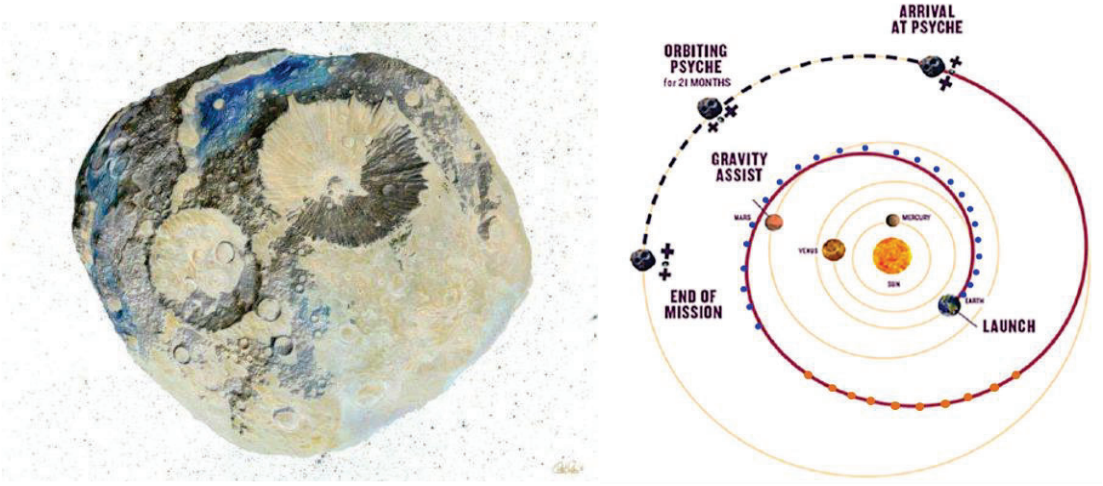

Figure 1, a) shows the Psyche Asteroid which consists of a major part of iron and nickel and might have been the core of an early planet. **b)** shows the trajectory of the Psyche spacecraft, the blue dots indicate the communication windows between the spacecraft and the NASA ground infrastructure, the orange dots indicate the communication windows between ESA's ground infrastructure and the spacecraft at distances between 1.25 and 2.75 AU. [3]

1.1 Further (historic) Missions with deep-space Optical Communication Demonstrations

Deep-space optical communication activities started at the Jet Propulsion Laboratory (JPL) in California with the Surveyor lunar lander in 1968 [4]. In 2013, the Lunar Laser Communication Demonstration (LLCD) demonstrated downlink throughputs of 622 Mb/s, in which ESA has participated establishing an optical link with its Optical Ground Station (OGS) at the Canary Islands [5]. Likewise, ESA was planning a Deep-Space Optical Communications System (DOCS) technology demonstration from the Sun-Earth Lagrange (L5) point, hosted by their Space Weather Mission spacecraft [6]. Also, the next Lunar Mission Artemis II will have a deep-space (lunar) optical communication demonstrator on board. In general, the huge amount of data collected by future missions are going to require fast down-link rates and thus optical communication [7] in addition to traditional radio frequency communication.

1.2 NASA JPL DSOC Terminal

The DSOC demonstration on the Psyche mission is led by NASA JPL and follows the last demonstration of optical communication in deep-space beyond the Moon, after NASA's experiment with its Messenger spacecraft orbiting Mercury, using the CCSDS standard for high photon-efficiency communication. Laser light from the DSOC terminal, which accommodates a 22-cm aperture on the spacecraft [8], will be received by ground stations equipped with single-photon detectors based on arrays of superconducting nanowires [9].

1.3 NASA JPL Ground Infrastructure

The Ground Laser Receiver from NASA will be realized by the Hale Telescope at Palomar Mountain in California and has an aperture of 5 m. The ground laser Transmitter will be at Table Mountain with a 1-meter aperture with an optical transmitter beam of up to 5 kW optical power.

1.4 ESA's Approach

While JPL has its own optical ground infrastructure to support the demonstration, ESA plans to complement it with a ground laser transmitter and receiver to demonstrate interoperability. ESA started three complementary activities to deploy and ensure data return from the Psyche spacecraft. One activity is concentrated on the ground laser transmitter. It provides a beacon laser towards the spacecraft and ensures back-pointing of the DSOC transmitter towards the European receiver site, while at the same time a modulation scheme provides data transfer from earth towards the spacecraft. The second activity focuses on the ground laser receiver, which collects data, coming from the spacecraft. The optical signal is received on single photon level and transferred into electrical signals by a superconducting nanowire single photon detector (SNSPD). The third activity is about a modem which transfers the electrical signal coming from the SNSPD into a data

return via the serially concatenated pulse position modulation (SC-PPM [2]) protocol. The three activities, their components and link budgets are described in the following sections.

2. GROUND LASER TRANSMITTER

The ground laser transmitter will provide information about the position of the ground station to the spacecraft via a high-power optical beacon in order to support pointing, acquisition and tracking. In addition to this beacon mode, the system will provide an uplink mode for ground-to-space data transfer.
Both laser systems modes will be high photon efficiency (HPE) compatible according to CCSDS 141.0-B-1 [10] and 142.0-B-1 [11]. A modulated multi-beam system architecture is foreseen. The pointing functionality will be tested with the Alphasat satellite, launched by ESA in 2013 and ever since being in a geostationary orbit [12]. Laser safety measures are implemented, and a laser launch system provides transmitter optics and infrastructure. For the final location of the transmitter different options are being considered. The candidate site at the time of writing is the Kryoneri Observatory [13] located in the northern Peloponnese, operated by the National Observatory of Athens.

2.1 Multi-Beam Laser System

The laser system will be based on multiple and spatially separated laser beams incoherently combined to achieve an overall average power level of approximately 7 kW and far-field scintillation minimization (e.g. by providing 10 laser beams, each with 700W average optical power). One assumes this multi-beam architecture averages out the irradiance fluctuations at the spacecraft. This approach also makes it possible to reach high average transmitting power by means of individual lower-power lasers that sum up in the far-field. The number of beams and output power of individual laser lines are still subject to final design. The laser source will be based on fiber technology and will operate at 1064 nm. System modularity will facilitate maintenance and ensure continued operability. In case of partial failure operations will not be interrupted but rather continue at reduced power levels. The modulation for uplink data transfer will be nested into the beacon signal with square wave pulses at a frequency of 3.8145 kHz [14] and a duty cycle of 50 %.

Intermediate Validation Scenario with Alphasat
The Ground Laser Transmitter will be commissioned using the geostationary satellite Alphasat, testing the blind pointing accuracy and the far field irradiance. For this reason, an additional modulation mode will also be implemented consisting in a beacon frequency of 1.0045 MHz and 50% duty cycle and left-handed circular polarized (LHCP); this makes reception possible on the Alphasat acquisition sensor.

Laser safety
The links will be operated in compliance with operational constraints imposed by aviation and local authorities concerning laser safety. The laser system will be interfaced to an aircraft detection system for in-sky laser safety. In case of predicted conjunction of air-traffic with laser hazard zone, the laser emission will be interrupted and resumed when conditions allow safe operations.

2.2 Laser Launch System

The Laser Launch System will perform the following functions:

- Launching the high-power beams delivered by the laser system by means of a telescope (including tracking mount) or an array of telescopes with near diffraction-limited performance
- Hosting laser system, telescope and auxiliary equipment
- Protecting the system components against environmental conditions
- Ensuring safe operations

A transportable, container-based, solution is baselined to allow faster system commissioning, installation and possible future relocation.
Different possibilities are being discussed for the system that will take care of pointing and transmitting the beacon laser beams. Namely, a main telescope with multiple sub-apertures to allow the launch into free space of the beams generated by the laser system or multiple launch telescopes held by a common pointing structure. The diameter of the sub-apertures or the aperture size of the launch telescopes envisaged for the first and second solution respectively, shall be smaller than typical r_0 at the installation site expected to be between 10 cm and 30 cm, to minimize the impact of atmospheric turbulence on the individual beams.

2.3 Uplink Budget Calculations

The required power to close the link, namely, scales with the square of the distance, over which the link is established as well as on the requested data rate, as follows:

$$P_{req} \propto D^2 \cdot T$$

where D and T respectively stand for the distance and the data rate. A trade-off between the distance and the data rate must then be done; the challenge being to transmit high data rates over long distances.

The table hereafter gives the main characteristics of the uplink:

Uplink	
Average Power [kW]	7
Wavelength [nm]	1064
Transmitter sub-aperture diameter [m]	~ 0.1
Receiver diameter [m]	0.22
Distance [Million km] **Distance [Astronomical Units - AU]**	**187 - 411** **1 .25 - 2.75**

The main function of the uplink beam is the so called “Beacon Mode”. The beacon transmitted from ground to space is used by DSOC to point back to the ground station on Earth with arcsec level precision. The received light at the spacecraft will be either only used to assist acquisition and tracking or also to receive telecommands from the ground. The required irradiance for tracking is 1 to 4pW/m² [15] on average. This value is determined by the detector characteristics and beacon angular position calculation algorithms [16].

The choice of the sub-aperture diameter is a trade-off between conflicting considerations: the larger the sub-aperture, the smaller the beam wander and the free-diffraction divergence of the beam. However, the divergence must be large enough compared to the beam wander and pointing accuracy of the system. Furthermore, the beam spread due to the turbulence increases with the sub-aperture diameter.

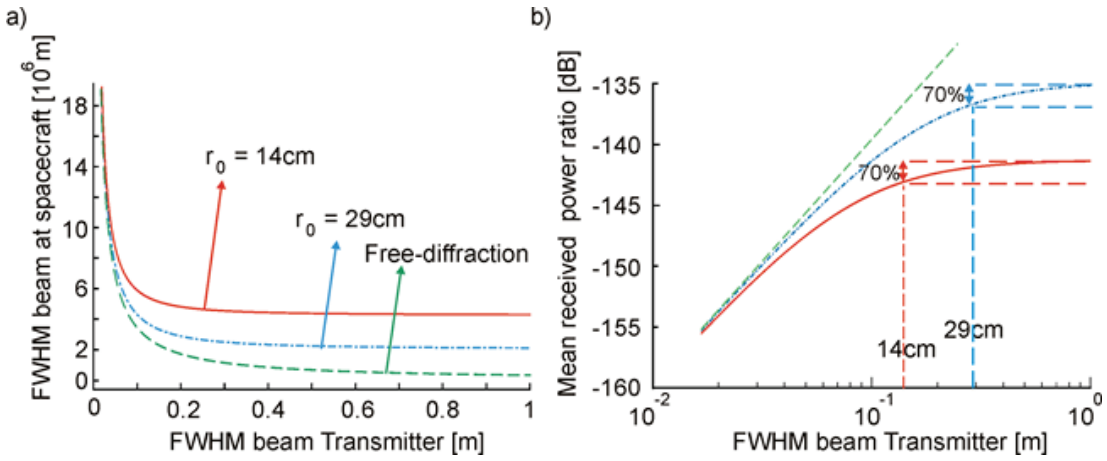

Figure 2 a) shows the diameter of the beam at the spacecraft, as a function of the transmitter beam diameter. **b)** shows the fraction of the mean power received on a 22 cm aperture (as that of the spacecraft) with respect to the total power. The curves are calculated for two different seeing conditions: 0.68 arcsec and 1.42 arcsec as reported in [18].

These values were measured to be the median seeing conditions at Kryoneri (900 m altitude) [13], respectively in July and October 2002 at 550nm, at zenith. It corresponds to approximately, $r_0 = 14$ cm and $r_0 = 29$ cm at a wavelength of 1064 nm and a zenith angle of 45°. The result for the diffraction limited scenario is also shown in the figure. One sees that for small transmitter diameters, the free-diffraction dominates over the atmospheric effects. When the FWHM diameter of the transmitted beam (enclosing 76% of the power) approximately equals the Fried parameter, the received irradiance reaches 70% of the maximum power. Beyond that value, the beam wander and beam spreading effects dominate; and the benefit of increasing the sub-aperture diameter is small.

Distance [AU]	**Irradiance at the spacecraft [pW/m²]**							
Fried parameter @1064, @45°	$r_0 = 14cm$				$r_0 = 29cm$			
Subaperture diameter d [cm]	5	10	15	20	5	10	15	20
1	25	42	45	45	36	100	152	180
1.5	11	19	20	20	16	45	68	80
2	6.2	11	11.3	11	9	25.5	38	45
2.5	4	6.8	7.3	7.1	5.8	16.3	24.4	28.8

Based on our preliminary design, the table gives the irradiances at the spacecraft for distances ranging between 1 to 2.5 Astronomical Units (AU). The total transmitted laser power is considered to be 7kW (700W per beam). The most pessimistic scenario (i.e that with the lowest irradiance) corresponds to a 5 cm diameter sub-aperture, at 2.5AU, for $r_0 =$ 14 cm. One notes that the required threshold to lock on the beacon (1 to 4pW/m²) is just reached and the performance can be improved with larger sub-apertures. The benefit is smaller for values above d=10 cm (at $r_0 = 14$ cm), which is consistent with the results shown on Figure 2. Note the outer scale was considered infinite for the calculations in this section.

3. GROUND LASER RECEIVER

The ground laser receiver will be installed at the Aristarchos telescope on mount Helmos in Greece. With an aperture of 2.3 m, it is the second single mirror largest telescope in Europe. It will be complemented with a super-conducting nanowire single photon detector (SNSPD) array, which is going to be developed and the most sensitive and accurate detection technology on the market. The pointing acquisition and tracking require a signal from the detectors, fast electronics and very accurate tracking. In the following subsections these components, the downlink link budget and the high photon efficiency modem are described in detail.

3.1 Ground Receiver Telescope

The Aristarchos telescope (Ritchey-Chretien design) was constructed by the German company Carl Zeiss GmbH and was inaugurated in the summer of 2007. It is located in the Northern Peloponnese at an altitude of 2340 m. The site is one of the darkest areas in Greece and Europe [1].

We expect the receiver demonstration period in the beginning of 2025. In this period (winter) we expect a decreased observability (25%) with respect to summer times (53%), because of potential clouds, humidity and wind. In favor play the longer nights in winter. The temperatures in Winter may range between -17 and 6 degrees Celsius during daytime and about 5 degrees less during nighttime [17].

The telescope's positional accuracy is better than 2 arcsec, while it can follow targets with a positional offset better than a fraction of an arcsec within an hour.

Figure 3. Aristarchos Telescope in Helmos, Greece.

3.2 Signal Photon Detection

The optical signal will be emitted from the DSOC terminal with an aperture of 22 cm, at a distance of up to 2.75 AU, (411 million kilometers). As a result, from gaussian beam divergence the beam diameter on Earth is in the order of 4000 km and the receiver telescope with its aperture of 2,3 meters will catch only a 10^{-12} part of the optical power, which has an average output of 4 W at the transmitter side. To detect that signal with a high timing precision we make use of a new technology based on superconducting nanowire structures. The detection principle is based on the transition of a nanowire from the superconductive to the resistive state upon the absorption of a single photon [18]. To achieve superconductivity the nanowires are cooled down to cryogenic temperatures of below 4-degree Kelvin. Using this technique, single photons in the NIR can be detected with efficiencies of above 85 percent and a timing precision of below 20 ps [19]. One photon at telecom wavelength (1550 nm) has an energy of about 10^{-19} Joule. Photons are required to be detected with a quantum efficiency of at least 85 % by each detector element (pixel). After detection the pixel is inactive for a few nanoseconds. To

ensure a high detection efficiency even for subsequent photons the optical beam should be spatially distributed on a detector array with 24 active pixels. Each pixel should be in the dimension of 10 µm. The total area should cover a circle with diameter 100 µm and have a filling factor of at least 50%. Dark count rates should not exceed 500 clicks per second per pixel and 10,000 cts/s for the whole array. The total detection efficiency including filling factor should exceed 50%.

3.3 Pointing, Acquisition and Tracking

An acquisition sensor will be used to center star-images to the previously determined single photon detector array and to calibrate the pointing offsets. Then the telescope will be navigated towards the trajectory of the satellite. For precise pointing the signal at 1550 nm wavelength will be spectrally filtered. Once the telescope is well aligned the light at the acquisition sensor will be at a minimum and the signal will be fully directed to the SNSPD array, which receives a maximum number of photons. This acquired signal will be used to track the satellite using a tip-tilt system, steered with positional information from the SNSPD array. Onedifficulty is that the electronics in the tracking loop need to be fast enough to be able to track the satellite (compensate tip/tilt) using only a single-photon level flux. The light traveling time takes twenty minutes at 2.75 AU and the relative speed of the satellite is 0.24 degree per minute. For that reason, the point ahead angle needs to be considered in the design which represents the offset between transmitter and receiver beam.

3.4 Down-link Budget Calculations

The following table provides the values of the contributions to the downlink budget:

Downlink budget contributors		
Parameter	**Value**	**Justification**
Signal transmission		
Transmitter power, average	4 W	Transmitter design
Transmitter wavelength	1550 nm	Transmitter design
Transmitter aperture diameter	0.22 m	Transmitter design
Transmitter optical losses	3.7 dB	Transmitter design
Pointing loss	2 dB	Estimate
Free–space path loss	117.33 - 124.18 dB	Calculated for link distance between 187 million km and 411 million km (1 .25 - 2.75 AU)
Atmospheric zenith transmittance	0.95	At 1550 nm, from literature
Scintillation penalty	0.1 dB	Estimate for 2.3-meter aperture
Receiver aperture diameter	2.28 m	HELMOS telescope
Receiver optical losses	6 dB	Estimate, losses between receiver aperture and photodetector, including central obscuration
Link margin	4 dB	Convention
Noise		

Transmitter extinction ratio	0.001	Transmitter design
Receiver filter bandwidth	2 nm	Requirement
Atmospheric Fried parameter	>0.1 m	Estimate, nighttime
Sky radiance at 1550 nm	1.2 μW cm^{-2} sr^{-1} μm^{-1}	From literature, nighttime
Background suppression	3 dB	Polarized transmitter
Photodetection		
Coupling loss	0.5 dB	Calculated
Detection efficiency	0.5	Requirement
Dark count rate	10^4 s^{-1}	Requirement
Implementation loss	1.5 dB	Estimate

The major contribution to the link loss is the free-space path loss caused by beam divergence over the range of link distances from 1.25 - 2.75 AU. A larger telescope aperture or a shorter transmission wavelength would decrease the beam divergence, thereby increasing the transmission gain, but the beam pointing would become commensurately more challenging. Further sources of losses are the transmitter and receiver optics and the atmosphere, through absorption and atmospheric turbulence. Taking all contributions into account, we calculate a signal flux at the photodetector of 40,000 ph s^{-1} at a range of 2.5 AU, and a background flux of around 13,000 ph s^{-1}.

Under these challenging link conditions, the strength of the SC-PPM coding and modulation format developed at JPL [20] and standardized by the Consultative Council for Space Data Systems (CCSDS) [2, 10, 11], becomes apparent. At a PPM order of M = 128 slots per symbol (plus 32 guard slots), 7 bits are encoded per PPM symbol. Operating with a slot width of 8 nanoseconds, repeat factor of 16, and a code rate of 1/3, the link can be closed at a data rate of 114 Kb s^{-1} [21].

The following table displays calculated signal and background count fluxes, and the link data-rates, together with the associated SC-PPM managed parameters, at a few selected link ranges and a link elevation of 20 degrees over the horizon.

Distance [AU]	**Signal flux [cts s^{-1}]**	**Background flux [cts s^{-1}]**	**M**	**Slot width [ns]**	**Repeat factor**	**Code rate**	**Downlink data rate [Mbps]**
1.25	1.67×10^5	1.40×10^4	128	8	8	2/3	0.456
1.5	1.16×10^5	1.39×10^4	128	8	8	2/3	0.456
1.75	8.53×10^4	1.36×10^4	128	8	8	1/3	0.228
2	6.53×10^4	1.36×10^4	128	8	8	1/3	0.228
2.25	5.16×10^4	1.35×10^4	128	8	8	1/3	0.228
2.5	4.18×10^4	1.35×10^4	128	8	16	1/3	0.114
2.75	3.45×10^4	1.34×10^4	128	8	16	1/3	0.114

The following plot shows the calculated data-rates over the range of link distances from 1.25 to 2.75 AU for three elevation angles of 20, 40 and 75 degrees.

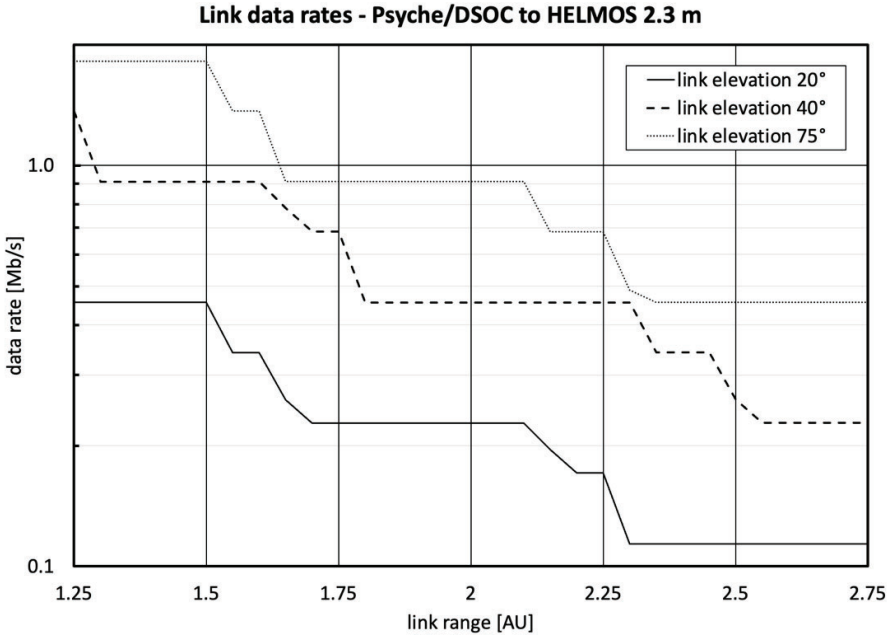

3.5 High Photon Efficiency Modem

As a key part of ESA optical ground segment for Psyche demonstration, a dedicated optical modem development is on-going. The HPE optical modem will ensure the reception of the downlink of the optical coding schemes SC-PPM waveform in the coding and synchronization as defined in the CCSDS blue book [10], as well as the physical layer of CCSDS [11]. For the uplink, the modem will support the transmission of the low-rate uplink data.

The HPE modem will interface with the combined tracking and data reception SNSPD detector, capable of detecting single photon events. The SNSPD detector will give a hard decision on the presence or not of photons into the considered slot. Moreover, the modem architecture supports four channels, foreseen for four quadrants of the SNSPD array. In order to ensure high data rate challenge for the downlink, the modem will implement a high-speed digitalization system ensuring in addition the support of low order PPM modulation and pulse width as low as 0.5 ns.

4. OUTLOOK AND CONCLUSION

Receiving optical signals from a deep-space spacecraft is a major challenge considering that one has to detect the signal at single photon level and compensate loss-free for atmospheric distortions. We carefully evaluated link budgets according to the SC-PPM standard and achieve data rates of several hundreds of kilobit per second for distances between 1.25 and 2.75 AU. During the development till 2025, we will refine taken assumptions and margins based on sub-system commissioning and select the most suitable optical communication parameters for the final link. This demonstration will further affirm collaboration between NASA and ESA in the domain of deep space optical communication and lead to validation of the inter-agency agreed CCSDS standards: paving the way for operational inter-operability and sharing of optical ground infrastructure.

4.1 Acknowledgements

We thank for helpful discussion with our industrial partners from OHB, Qtlabs, SA Synopta, Single Quantum, QSYS and Safran.

Dimitrios Antsos' and Abhijit Biswas' contributions to this paper were supported by the Jet Propulsion Laboratory, California Institute of Technology, under a contract with the National Aeronautics and Space Administration (80NM0018D0004).

5. REFERENCES

[1] https://helmos.astro.noa.gr/
[2] B. Moision and J. Hamkins, "Coded Modulation for the Deep-Space Optical Channel: Serially Concatenated Pulse-Position Modulation", IPN Progress Report 42-161 (2005).
[3] https://psyche.asu.edu/
[4] H. Hemmati, "Deep space optical communication", Deep Space Communications and Navigation Serie, Jet Propulsion Laboratory (2005).
[5] Z. Sodnik, H. Smit, M. Sans, D. Giggenbach, P. Becker, R. Mata Calvo, I. Zayer, M. Lanucara and K.-J. Schultz, "Results from a Lunar Laser Communication Experiment between NASA's LADEE Satellite and ESA's Optical Ground Station", International Conference on Space Optical Systems and Applications (2014).
[6] Z. Sodnik et al.; "Deep-space Optical Communication System (DOCS) for ESA's Space Weather mission to Lagrange orbit L5"; 2017 IEEE International Conference on Space Optical Systems and Applications (2017).
[7] N.K. Lyras, A.D. Panagopoulos and P.-D. Arapoglou, "Deep Space Optical Communication Link Engineering: Sensitivity Analysis", IEEE Aerospace and Electronic Systems Magazine **34**, 11 (2019).
[8] L. J. Deutsch, "Towards deep space optical communications", Nature Astronomy **4**, 907 (2020).
[9] B. E. Vyhnalek, J. N. Downey, and S. A. Tedder; "Single-Photon Counting Detector Scalability for High Photon Efficiency Optical Communications Links"; NASA Glenn Research Center (2020)
[10] Optical Communications Physical Layer; Recommended Standard; CCSDS 141.0-B-1 (2019)
[11] Optical Communications Coding and Synchronization: Recommended Standard CCSDS 142.0-B-1 (2019).
[12] Z. Sodnik, C. Voland, J. Perdigues, E. Fischer, K. Kudielka, R. Czichy, "Optical feeder-link between ESA's optical ground station and Alphasat", International Conference on Space Optics - ICSO 2020; 1185218 (2021)
[13] https://kryoneri.astro.noa.gr/en/
[14] Orbit Data Messages: Recommended Standard CCSDS 502.0-B-2 (2009)
[15] E. Alerstam, K. Andrews, M. Srinivasan, A. Wong; "The effect of photon counting detector blocking on centroiding for deep space optical communications", SPIE LASE (2018)
[16] M. Srinivasan, K. S. Andrews, W. H. Farr, A. Wong; "Photon counting detector array algorithms for deep space optical communications", SPIE LASE (2016)
[17] P. Hantzios, I. Alikakos, "Technical Report 1: Characterization of the observing conditions of the Helmos Observatory", IAASARS (2019)
[18] W. Zhang, J. Huang, C. Zhang, L. You, C. Lv, L. Zhang, H. Li, Z. Wang and X. Xie; "A 16-Pixel Interleaved Superconducting Nanowire Single-Photon Detector Array With A Maximum Count Rate Exceeding 1.5 GHz"; IEEE Transactions on Applied Superconductivity **29**, 5 (2019)
[19] J. Chang, I. E. Zadeh, J. W. N. Los, J. Zichi, A. Fognini, M. Gevers, S. Dorenbos, S. F. Pereira, P. Urbach, and V. Zwiller; "Multimode-fiber-coupled superconducting nanowire single-photon detectors with high detection efficiency and time resolution"; Applied Optics **58**, 36 (2019)
[20] J. Hamkins; High Photon Efficiency (HPE) Recommendation Status; JPL (2016)
[21] M.L. Vatsia; Atmospheric Optical Environment; Research and development technical rept.; p. 22 (1972)